

Observed Scattering into a Dark Optical Vortex Core

David Palacios, David Rozas,* and Grover A. Swartzlander, Jr.

Optical Sciences Center, University of Arizona, Tucson, Arizona 85726

(Received 4 December 2001; published 25 February 2002)

The dark core of an optical vortex was used to detect on-axis, forward-scattered light from a colloidal solution in the single and multiple scattering regimes. Using no adjustable parameters we obtain good agreement with a concentration-dependent scattering model.

DOI: 10.1103/PhysRevLett.88.103902

PACS numbers: 42.25.Fx, 42.15.Eq, 42.25.Kb, 82.70.Dd

An optical vortex is characterized by a dark channel of destructive interference that nulls coherent light [1]. Optical vortices occur naturally in cylindrical beams [2] and in scattered light [3,4]. They may also be synthesized using computer generated holograms [5–7] or diffractive optical elements [8,9]. In all these cases a vortex is produced when the scalar phase around the dark vortex core in the transverse plane is azimuthally harmonic—similar to an orbital angular momentum state. The propagating phase fronts are helical, and unless acted upon by a scattering body, a vortex in a coherent beam will propagate to infinity. Scattering, however, may superimpose other modes into the dark vortex core region, shifting or brightening the core if the light is, respectively, coherent or incoherent. The core may therefore be used as a window for a variety of applications to detect scattered light without the blinding effects of the unscattered coherent source [10]. Applications of this scheme may include the detection of objects near bright sources (e.g., extra-solar planets, zodiacal dust, missiles with attached plumes, or defects in laser optics), optical tomography, or measurement techniques based on light scattering.

When a laser beam shines through particles larger than the wavelength, light is scattered in all directions; however, the most intense scattering usually occurs in the forward direction [11]. Light scattered along the optical axis is often difficult to distinguish from the superimposed unscattered laser beam, especially when there is a dilute concentration of weak scatterers. In typical scattering experiments used to determine particle sizes, the intensity of the zero angle scattered light is orders of magnitude smaller than the beam intensity, and the signal is essentially lost in the glare of the beam. Nonexistent or inaccurate zero angle scattering data pose problems for techniques that use the inverse scattering method to determine particle size distributions [12,13]. Thus a technique that nulls the coherent on-axis unscattered radiation may allow more accurate particle size determinations. Interferometric nulling techniques [14,15] combining two or more beams have been used to null a bright on-axis coherent source for scattering measurements or planet detection, but these systems are sensitive to vibrations and alignment errors. In comparison, the nulling produced by a vortex phase mask, as

discussed in this Letter, is relatively immune to vibrations, and sensitive optical alignments are not required.

In cylindrical coordinates, a single ideal optical vortex in the center of a beam propagating in the z direction may be written

$$E(r, \phi, z) = A(r, z) \exp(im\phi) \exp(-ikz), \quad (1)$$

where $A(r, z)$ is a circularly symmetric amplitude function, $k = 2\pi/\lambda$ is the wave number of a monochromatic field of wavelength λ , and m is a signed integer known as the topological charge. For convenience we assume m is positive. Total destructive interference occurs at $r = 0$ when m is a nonzero integer, and thus Eq. (1) implies that the diffracting envelope function $A(r, z)$ remains zero valued at $r = 0$ as the beam propagates [7]. In this Letter we examine the case where the envelope initially has a pillbox profile, except for a zero at $r = 0$. In the far-field region (or in the focal plane of a lens) the vortex core diffracts to a size that is on the order of the beam size. Within the far-field core the fraction of power transmitted through a centered aperture of radius $r < R_{\text{diff}}$ decreases as roughly $(r/R_{\text{diff}})^{1.44+1.82m}$, where R_{diff} is the radial size of the Airy disk [10]. The darkness in the core is therefore enhanced as the topological charge is increased. For noninteger values of m , a radially diffracting line may accompany the vortex, owing to a phase discontinuity along an edge.

A beam having a planar ($m = 0$) wave front may be converted into a vortex beam by transmitting the beam through a transparent mask having a thickness,

$$d = d_0 - m\lambda_0\phi/2\pi(\tilde{n}_2 - \tilde{n}_1), \quad (2)$$

where d_0 is the nominal thickness, λ_0 is the wavelength for which the mask is intended, \tilde{n}_2 is the refractive index of the mask, and \tilde{n}_1 is the index of refraction of the surrounding medium. Discrete rather than continuous diffractive optical elements are more common, owing to the availability of precise lithographic facilities. Our mask, fabricated by the Consortium for Optical and Optoelectronic Technologies for Computing [16], resembled a spiral staircase having eight steps, each differing in phase from its adjacent neighbor by $2\pi/8$. The mask was designed to produce a vortex of charge $m = 1$ at $\lambda_0 = 850$ nm at an air-fused silica interface.

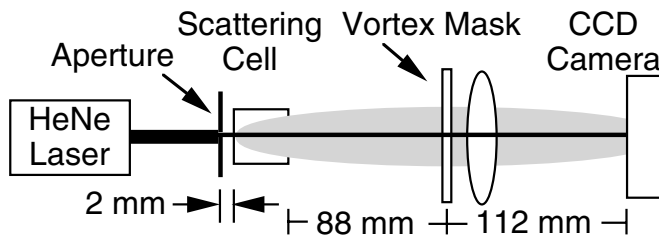


FIG. 1. Schematic diagram of the experiment showing light from a laser beam passing through an $25 \mu\text{m}$ diameter aperture, a 10 mm long scattering cell, a vortex phase mask, and an imaging lens arranged for unity magnification onto a low noise digital astronomy camera.

The mask, placed behind a scattering cell as shown in Fig. 1, equally affects the phase of the scattered and unscattered light, but only the spatially coherent components develop the intended vortex core. Assuming the incident beam is spatially coherent, the field transmitted through both the scattering cell and an ideal phase mask may be written in the form of Eq. (1):

$$E(r, \phi, z) = \{A_{\text{unsc}}^{\text{coh}}(r, z) + A_{\text{sc}}^{\text{coh}}(r, \phi, z) + A_{\text{sc}}^{\text{incoh}}(r, \phi, z)\} \times \exp[-im(\lambda_0/\lambda)\phi], \quad (3)$$

where sc (unsc) and coh (incoh), respectively, indicate scattered (unscattered) and coherent (incoherent) light. We ignore the phase factor, $\exp[-ikn_2d_0 - ikn_1(z - d_0)]$. The complex scattered amplitude functions have spatial distributions that depend on the shape and concentration of scatterers, and they are generally time dependent, e.g., owing to moving particles or a finite coherence time of the laser [17].

For simplicity we assume the intensity centroids of each scattered beam coincide with the optical axis where $A_{\text{unsc}}^{\text{coh}}(r = 0, z) = 0$. The complex speckle field, $A_{\text{sc}}^{\text{coh}}$, formed from the coherent superposition of fields from many scatterers, may be highly structured. The vortex position may be shifted by intensity and phase gradients of the speckle; however, this effect may be negligible if the coherence area of $A_{\text{sc}}^{\text{coh}}$ in the detection plane is smaller than a pixel. Thus we ignore $A_{\text{sc}}^{\text{coh}}$ below. The term $A_{\text{sc}}^{\text{incoh}}$ is a random variable. For the case $m(\lambda_0/\lambda) = \pm 1$, the resulting time integrated intensity in the vicinity of the vortex core may be written

$$\langle |E(r, \phi, z; t)|^2 \rangle = \langle |a_{\text{unsc}}^{\text{coh}}|^2 \rangle (r/w)^2 + \langle |A_{\text{sc}}^{\text{incoh}}|^2 \rangle + I_0^{\text{incoh}}, \quad (4)$$

where we assume $\langle A_{\text{sc}}^{\text{incoh}} \rangle = 0$ and $A_{\text{unsc}}^{\text{coh}} = a_{\text{unsc}}^{\text{coh}} r/w$ for $r \ll w$, where w is the characteristic size of the beam, and we have added the term I_0^{incoh} which is attributed to incoherent light from the laser source. Equation (4) shows that the incoherently scattered radiation can be directly measured by placing a small detector at the vortex center, $r = 0$, when $I_0^{\text{incoh}} \ll \langle |A_{\text{sc}}^{\text{incoh}}|^2 \rangle$. This result may be

generalized for a vortex core translated to any point in the beam, thereby allowing the angular measurement of the scattering spectrum.

Yang *et al.* estimated the far-field concentration dependent incoherent scattering distribution for a few scattering events [18], which we express as

$$\langle |A_{\text{sc}}^{\text{incoh}}|^2 \rangle / I_0^{\text{coh}} = \sum_j (C_j a_j / j!) (\rho / \rho_0)^j \exp(-\rho / \rho_0) \times \exp[-2.69 a_j (wr/\lambda z)^2], \quad (5)$$

where j is the number of times the light is scattered before emerging from the cell, the coefficients $0 \leq C_j \leq 1$ are coherence factors determined from experimental data, $a_j = (1 + 0.273 j w^2 / w_s^2)^{-1}$, $\rho_0 = (\pi R^2 L)^{-1}$ is the scattering extinction parameter (L is the length of the cell, and R is the particle radius), w is the radial size of the aperture near the input face of the cell, $w_s = R n_2 / n_1$ (n_2 / n_1 is the ratio of refractive indices of the particle and the host medium), and I_0^{coh} is the scatter-free on-axis intensity when the phase mask is removed, r is the distance from the optical axis in the transverse far field plane, and z is the far-field distance from the aperture to the object plane—here the output face of the cell.

To demonstrate the coherence filtering ability of a vortex phase mask, a HeNe laser beam ($\lambda = 632.8 \text{ nm}$) was passed through a scattering cell containing an aqueous suspension of $2R = 2.25 \mu\text{m}$ diameter polystyrene spheres ($n_2 = 1.59, n_1 = 1.33, w_s = 1.34 \mu\text{m}$). The concentration of spheres, ρ , was varied from 0 to 2.3×10^8 spheres/ml in the $L = 10 \text{ mm}$ long cell. A 10 nm laser filter was placed at the output of the laser to reject broadband radiation from the plasma tube. A $2w = 25 \mu\text{m}$ diameter aperture was placed near the input face of the cell, thereby achieving a value of $a_1 = 0.04$. (Note: a larger aperture produces a smaller fraction of scattered light, whereas a smaller aperture results in a weaker signal.) The output plane of the scattering cell was imaged without magnification with a 50 mm focal length, $f/2$ lens, onto a Meade Pictor Model 416XT 16 bit digital camera having $9 \mu\text{m} \times 9 \mu\text{m}$ pixels. To take advantage of the full dynamic range of the camera, time exposures varied from $T_{\text{exp}} = 30 \text{ s}$ for strong scattering to 1 s for weak scattering. To achieve a large diffracted vortex core in the detection plane, the vortex phase mask was placed near the imaging lens.

Samples of the recorded images are shown in Fig. 2. Note that dark frame images have been subtracted to increase the accuracy of our data. The scatter-free case, $\rho = 0$, in Fig. 2(a) shows a vortex core at the origin [even though $|m|(\lambda_0/\lambda)$ is greater than unity], as well as radial diffraction lines caused by the discrete phase steps on the mask. We confirmed the vortex nulling effect predicted in Ref. [10] by determining the ratio of power in the core to that of the total beam: $(\delta P / P_{\text{total}})_{\text{exp}} = 10^{-5}$, whereas $(\delta P / P_{\text{total}})_{\text{theory}} = 3 \times 10^{-6}$. In the strong scattering case, $\rho = 2.3 \times 10^8 \text{ cm}^{-3}$, diffuse light fills the

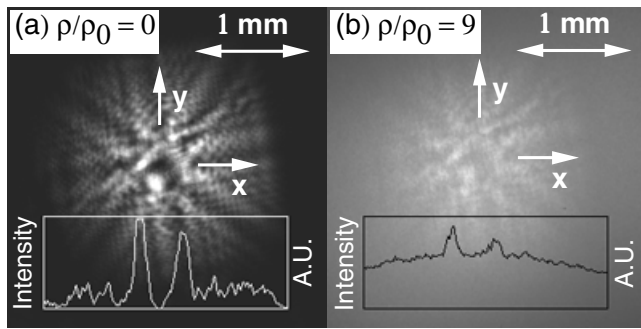


FIG. 2. Recorded intensity distributions for (a) zero scattering and (b) high scattering. Superimposed line plots show intensity profiles, $I(x, y = 0)$, through the vortex cores. The intensity nearly vanishes in (a), but is nonzero due to zero-angle scattering in (b).

image in Fig. 2(b). Line plots superimposed on the images depict the intensity distributions through the vortex and across the beam. We note that speckle from coherent scattering is not seen owing to long integration times and an average speckle area about the size of a pixel.

To quantify the amount of light scattered into the vortex core we determined the average number of counts per pixel per second, κ , within a 3×3 array of pixels centered on the vortex at $r = 0$. A mean value was obtained by averaging over three repeated measurements at a given concentration:

$$\bar{\kappa}_\rho = T_{\text{exp}}^{-1} \sum_{i,j,k=1}^3 (1/27)n_k(x_i, y_j), \quad (6)$$

where n_k is the number of photons counted at the pixel labeled by (i, j) . For comparison we also measured the average counts per pixel per second, \bar{K}_ρ , over a large area of the beam. The ratio $\bar{\kappa}_\rho/\bar{K}_{\rho=0}$, which may be compared with Eq. (5), is shown in Fig. 3 as a function of the normalized particle concentration ρ/ρ_0 , where $\rho_0 = 2.5 \times 10^7 \text{ cm}^{-3}$. As expected from Eq. (5), the relative intensity of the core initially increases as ρ/ρ_0 increases, and then decreases as scattering attenuates the transmitted light. The solid line in Fig. 3 represents the calculated values of Eq. (5). The coefficient C_0 is assigned the measured values $\bar{\kappa}_{\rho=0}/\bar{K}_{\rho=0} = 0.033$. The scattered light is expected to be incoherent, and thus we set $C_{j>0} = 1$. The summation in Eq. (5) may be terminated at $j = 3$ since the model is valid for only a few scattering events. Thus, using no adjustable parameters, we find good agreement between our data and the predicted values in Eq. (5).

In conclusion, we have used an optical vortex phase mask to null unscattered coherent light and measure incoherent scattered light along the optical axis. The concentration dependent scattering intensity agreed with a theoretical model for multiple scattering. This novel technique may be generalized to measure the scattering spectrum by translating the phase mask across the scattered beam. Our measurements confirm that an optical vortex may be used as a window to measure a weak

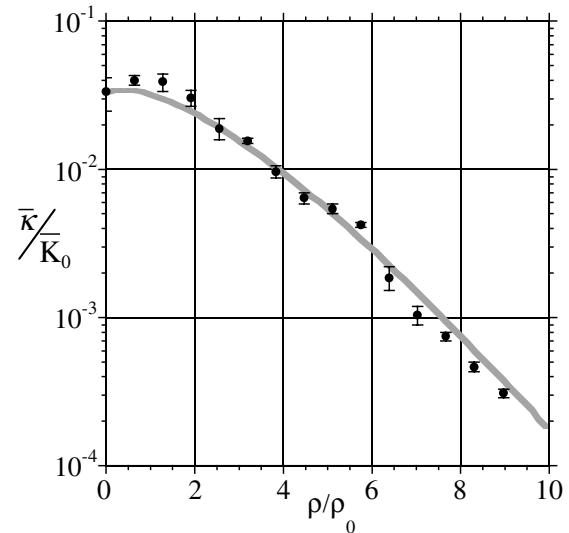


FIG. 3. Zero-angle scattered light as a function of scattering concentration where $\rho_0 = 2.5 \times 10^7 \text{ cm}^{-3}$, $\bar{\kappa}$ is proportional to the average intensity over a small region of the vortex core, and \bar{K}_0 is proportional to the average intensity across a large area of the beam at $\rho = 0$. The experimental data (circles) agrees well with a multiple scattering theoretical model (line).

optical signal in the presence of an intense superimposed coherent beam of light.

We thank Kannan Raj of George Mason University for coordinating the diffractive optics foundry. This work was supported by the Research Corporation (Cottrell Scholar Program), the University of Arizona, the National Science Foundation, and the Defense Advanced Research Project Agency.

*David Rozas made contributions as a graduate student at Worcester Polytechnic Institute, Worcester, MA. He is now at Analogic, Corp., Peabody, MA.

- [1] *Optical Vortices*, edited by M. Vasnetsov and K. Staliunas, Horizons in World Physics, Vol. 228 (Nova Science, Huntington, NY, 1999).
- [2] S. Ramo, J.R. Whinnery, and T. Van Duzer, *Fields and Waves in Communication Electronics* (Wiley, New York, 1965).
- [3] J.F. Nye and M.V. Berry, Proc. R. Soc. London Ser. A **336**, 165 (1974).
- [4] N.B. Baranova, B. Ya. Zel'dovich, A.V. Mamaev, N.F. Pilipetski, and V.V. Shkunov, Pis'ma Zh. Eksp. Teor. Fiz. **33**, 206 (1981) [JETP Lett. **33**, 195 (1981)].
- [5] V. Yu. Bazhenov, M. V. Vasnetsov, and M. S. Soskin, Pis'ma Zh. Eksp. Teor. Fiz. **52**, 1037 (1990) [JETP Lett. **52**, 429 (1990)].
- [6] N.R. Heckenberg, R. McDuff, C.P. Smith, and A.G. White, Opt. Lett. **17**, 221 (1992).
- [7] Z. S. Sacks, D. Rozas, and G. A. Swartzlander, Jr., J. Opt. Soc. Am. B **15**, 2226 (1998).
- [8] M. W. Beijersbergen, R. P. C. Coerwinkel, and J. P. Woerdman, Opt. Commun. **112**, 321 (1994).

- [9] F.B. Colstoun, G. Khitrova, A. V. Fedorov, T.R. Nelson, C. Lowery, T.M. Brennan, B.G. Hammons, and P.D. Maker, *Chaos Solitons Fractals* **4**, 1575–1596 (1995).
- [10] G. A. Swartzlander, Jr., *Opt. Lett.* **26**, 497 (2001).
- [11] W. Grandy, Jr., *Scattering of Waves from Large Spheres* (Cambridge University Press, Cambridge, U.K., 2000).
- [12] M.Z. Hanson, *Appl. Opt.* **19**, 3441 (1980).
- [13] Joseph H. Koo and E. Dan Hirtleman, *Appl. Opt.* **31**, 2130 (1992).
- [14] L.G. Kazovsky and N.S. Kopeika, *Appl. Opt.* **22**, 706 (1983).
- [15] J.R.P. Angel and N.J. Woolf, *Astrophys. J.* **475**, 373 (1997).
- [16] This diffractive optical element foundry was sponsored by DARPA in 1995–1996, in cooperation with Honeywell International, Inc. and George Mason University.
- [17] A. Ishimaru, *Wave Propagation in Random Media*, the IEEE/OUP series on electromagnetic wave theory (Academic Press, New York, 1978).
- [18] Changhuei Yang, Kyungwon An, Lev T. Perelman, Ramachandra R. Dasari, and Michael S. Feld, *J. Opt. Soc. Am. A* **16**, 866 (1999).